Modeling of Ground-Penetrating Radar Wave Propagation in Pavement Systems

CHUN LOK LAU, TOM SCULLION, AND PAUL CHAN

In recent years considerable attention has been focused on the use of ground-penetrating radar (GPR) to detect a variety of pavement problems. The results to date have been mixed. Information on the electrical properties of highway materials is limited as is the ability to model the propagation of electromagnetic waves in a pavement system. A forward model capable of simulating the signature of GPR waveforms is proposed. A monostatic 1 GHz GPR is used in this study. The pavement system is modeled as a layered medium comprising flat parallel layers of pavement materials laminated together. Physical laws governing electromagnetic wave propagation inside the layered medium are used to calculate the attenuation, dispersion, reflection, and transmission encountered by the pulse. Major reflection paths and some multiple reflection paths are selected that begin from the open tip of the antenna, penetrate into the pavement, and reach the pavement surface again. The analysis is performed in the frequency domain. The transmitted pulses are traced through each of these paths one at a time. The resultant echoes at the pavement surface are then positioned and superimposed together according to the time required for the pulse to travel each of the selected paths. A synthetic waveform is thus formed. This process is called forward modeling. The forward model is tested on data collected on experimental pavements of known layer thicknesses and types. Reasonable agreement was achieved between theoretically calculated and field-measured GPR traces. In predicting the amplitude of the waves reflected from layer interfaces average errors of less than 9 percent were calculated. The error in estimating the time delays between peaks was less than 2.5 percent. More work is required, particularly in the area of measuring the complex dielectric properties of paving materials under a range of operational temperature and moisture conditions.

In recent years several investigators have attempted to use ground-penetrating radar (GPR) to detect subsurface problems in pavement systems. Much of the initial work was focused on manual interpretation of multiple GPR traces collected along a highway. The traces were often color coded, and an expert was needed to locate the problem areas. Sometimes the approach worked; other times poor results were obtained. Highway department personnel who evaluated the technology recognized potential but were often disappointed by the manual interpretation system.

Only relatively recently have automated procedures been applied to estimating layer thicknesses (*1*) and detecting voids (*2*,*3*). These procedures model the pavement as a multilayered system and apply the laws of electromagnetic wave propagation to interpret the results from a single GPR-reflected signal. If a single reflected trace cannot be interpreted, there is little hope of obtaining quantifiable information from multiple traces. It is the authors' opinion that GPR technology shows potential for highway applications. However, the authors' knowledge of the required electrical properties of pavement materials is limited. In addition, few models exist that adequately explain how a GPR wave propagates through a layered system of different complex dielectrics. Such a model is proposed in this paper.

Texas Transportation Institute, Texas A&M University, Room 503B CE/TTI Building, College Station, Tex. 77843-3135.

A pavement system is modeled as a layered medium consisting of layers of distinct pavement materials. To GPR signals, different pavement materials are distinguishable electrically in terms of relative permittivity (i.e., dielectric constant), magnetic permeability and conductivity. In highway applications the parameter that has the most influence on these properties is the moisture content of the pavement layer. A list of relative dielectric constants of typical pavement materials measured at room temperature at 1 GHz follows:

- Asphalt: 2–6,
- Crushed limestone: 3–9,
- Hot-mix asphalt: 4–6,
- Concrete: 6–9,
- Air: 1, and
- Water: 81.

Clearly the addition of moisture to a pavement layer will significantly increase the dielectric constant of that layer.

For analysis purposes, a simulation model capable of predicting the signature of a GPR waveform collected under certain pavement subsurface conditions is desirable. Modeling offers several advantages. For example, suppose a section of pavement with a 5-in. layer of Type A asphalt, a 10-in. layer of Type B base, and Type C subgrade is studied by GPR, and a simulated signature of the GPR waveform is obtained successfully. To predict the GPR signature of a pavement with the same materials and with the presence of an air- or water-filled void, it is a simple matter of adding a layer of air or water to the pavement model and to repeat the same simulation procedures. Additionally, a realistic forward model of a GPR trace can potentially provide a way to estimate both the thickness and material properties of each layer in the pavement structure. The idea is to use an iterative procedure that varies the unknown parameters to minimize the sum of squared error between actual and calculated traces.

In this paper a simulation model is established for the prediction of GPR signature as would be collected from a pavement with specified subsurface conditions. The result of a simulation example will be given to demonstrate the feasibility of modeling in assisting pavement subsurface condition assessment. The intermediate results of the modeling process

will also be presented to aid understanding of the propagation characteristics of the GPR signal in a pavement system.

GPR AND BACKGROUND OF ELECTROMAGNETIC THEORY (*4*)

Two types of GPR are commercially available: monostatic and bistatic. As shown in Figure 1, the former uses a single antenna for transmission and reception. The latter uses two separate but identical antennas.

For this study, a Penetradar model PS-24 monostatic GPR (pulse − width = 1 nsec; center frequency = 1 GHz) was used. A typical trace from this radar on a pavement is shown in Figure 2. The amplitudes are those reflected from significant layer interfaces. The time delays are related to layer thicknesses and will be discussed further. The aim of this study is to build a theoretical model to simulate reflected GPR traces.

GPR works according to the pulse-echo principle. A narrow electromagnetic pulse is generated by the transmitter and radiated toward the pavement through the antenna. In many cases, the wavefront of the transmitted pulse reaching the pavement surface is approximately a plane wave. Below this surface is a lossy inhomogeneous medium made of pavement materials. However, to a 1-ft radar wave, the medium may appear homogeneous. The propagation of a plane wave along the z-direction, perpendicular to the surface, in a homogeneous medium is governed by the wave equation (*5*):

$$\frac{\partial^2 E}{\partial z^2} = -\omega^2 \mu \varepsilon E \tag{1}$$

where

E = Re[$E_0 \exp(j\omega t)$] = sinusoidal time varying electric field vector (V/m),
E_0 = amplitude of the electric field vector (V/m),
ω = angular frequency (rad/sec),
z = distance along the propagation direction (m),
μ = magnetic permeability,
$\varepsilon = \varepsilon' - j\varepsilon''$ = complex permittivity (F/m),
$\sigma = \sigma' + j\varepsilon''$ = conductivity (mho/m).

A solution for E in Equation 1 is

$$E = E_0 e^{-jkz} \tag{2}$$

with propagation constant

$$k = \omega\sqrt{\mu\varepsilon\,(1 - j\tan\delta)} \tag{3}$$

The loss tangent is defined by

$$\tan\delta = \frac{\frac{\sigma}{\varepsilon_0} + \omega\,\varepsilon_r''}{\omega\,\varepsilon_r'} \tag{4}$$

where

$\varepsilon_0 = 8.854 \times 10^{-12}$ = permittivity of free space (F/m),
$\varepsilon_r' = \varepsilon'/E_0$ = real part of the relative permittivity, and
$\varepsilon_r'' = \varepsilon''/\varepsilon_0$ = imaginary part of the relative permittivity.

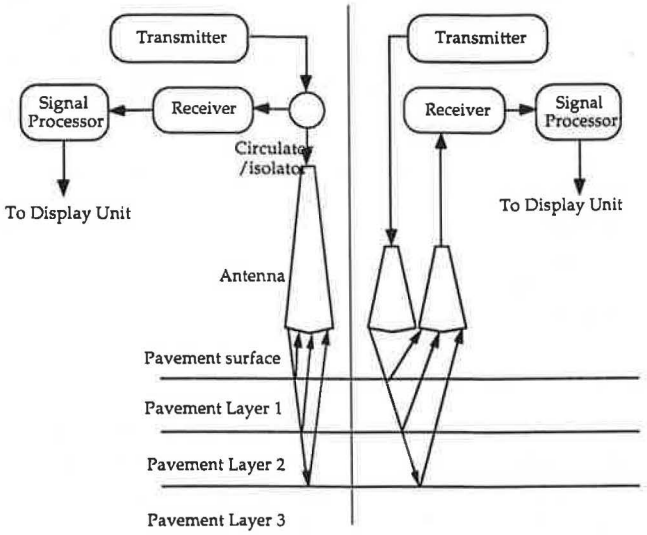

FIGURE 1 Monostatic (*left*), and bistatic (*right*) GPR.

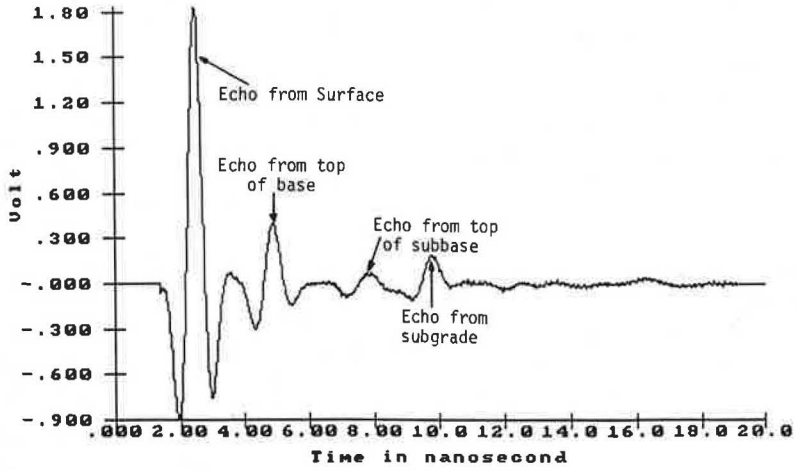

FIGURE 2 Actual GPR traces from four-layered pavement at TTI Research Annex.

If the real and the imaginary parts of jk are separated and the attenuation parameter α and the phase parameter β are written as

$$\alpha = \omega\sqrt{\frac{\mu\varepsilon}{2}\left(\sqrt{(1 + \tan^2\delta} - 1\right)}\left(\frac{\text{neper}}{m}\right) \quad (5)$$

$$\beta = \omega\sqrt{\frac{\mu\varepsilon}{2}\left(\sqrt{1 + \tan^2\delta} + 1\right)}\left(\frac{\text{radian}}{m}\right) \quad (6)$$

Equation 2 can be rewritten as

$$E = E_0\, e^{-\alpha z}\, e^{-j\beta z} \quad (7)$$

The amplitude of the GPR pulse decreases as it propagates in the material medium, and the pulse shape is distorted because of the nonlinear phase term βz. Equations 5 and 6 will be used in forward modeling to calculate the attenuation and the dispersion caused by the lossy characteristics of the layered medium.

Equation 7 shows that a negative value of α will diminish the amplitude of E of the wave traveling in the z-direction, and βz is a nonlinear phase term that distorts the shape of the signature in time domain. These phenomena will be shown later.

A GPR pulse propagating inside the multilayer pavement system will encounter the interfaces between the pavement layers where reflection and transmission take place. The parameters that determine the amount of the energy that is reflected back toward the antenna and the remaining portion that travels downward toward the next interface are the reflection and transmission coefficients, respectively. They are defined for Layers 1 and 2 as follows:

$$R \equiv \frac{E_r}{E_i} = \frac{\mu_2 k_1 - \mu_1 k_2}{\mu_2 k_1 + \mu_1 k_2} \quad (8)$$

$$T \equiv \frac{E_t}{E_i} = \frac{2\mu_2 k_2}{\mu_2 k_1 + \mu_1 k_2} \quad (9)$$

For waves propagating through a multilayered medium, the amplitude of the reflected electric field and transmitted electric field can be expressed in terms of the reflection and transmission coefficients, in the nth layer

$$E_r(n) = R(n)\, E_i(n) \quad (10)$$

$$E_t(n + 1) = T(n)\, E_i(n) \quad (11)$$

where the subscript n refers to the nth interface in a multilayer pavement system. Only the electric field is considered here because the receiver electronics in a GPR detects and processes only voltage waveforms.

Both the reflected and the transmitted energy are attenuated and their spectral characteristics altered by dispersion as determined by Equations 5–7. These events take place at each interface of the pavement system. The pulse is traced through selected paths, and events occurring along the way are calculated. A synthetic waveform can be constructed on the basis of knowledge of the events and times of occurrence.

FORWARD MODELING

Assumptions

Forward modeling is based on the following assumptions:

1. Parallel and planar layers. This assumption is generally true for typical pavement systems. The subsurface interfaces may be considered as parallel and smooth for a microwave energy of a wavelength of 1 ft (30 cm).
2. Plane wave. For monostatic GPR, normal incidence and reception is easily achieved. There are good reasons to assume that the wavefront does not deviate significantly from a plane wave. The only obvious cause for deviation from a plane wave will be the geometrical spreading of the wavefronts shown in Figure 3. This may be accounted for by simple manipulation: (a) measure the length of the horn antenna (L), (b) divide the distance traveled by a reflection or multiple reflection event by L and add 1 to the result, and (c) divide the amplitude of the final wavelet amplitude of the corresponding reflection event by the number obtained in (b).

Selected Paths and Events

The models used in this program are an adaption of those proposed by Duke in 1990 (*6*). The selected paths of the radar pulse begin at the air-pavement interface and continue into the subsurface of a four-layer medium as shown in Figure 4. The angles of incidence are zero at all interfaces. Oblique rays used are for illustration purpose only. Multiple reflections occur, and their electric field amplitudes may be comparable with that of a major reflection from lower layers. Consequently, their use must be accounted for in the theoretical

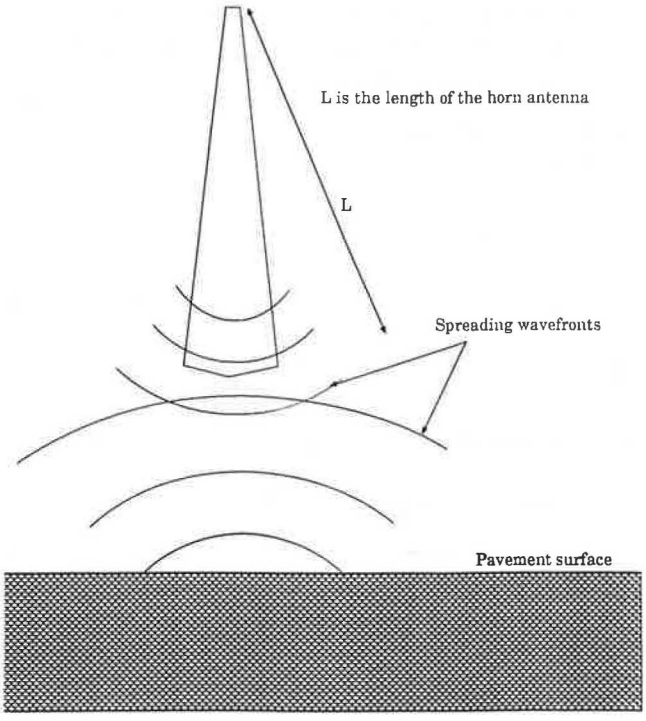

FIGURE 3 Geometric spreading of wavefronts.

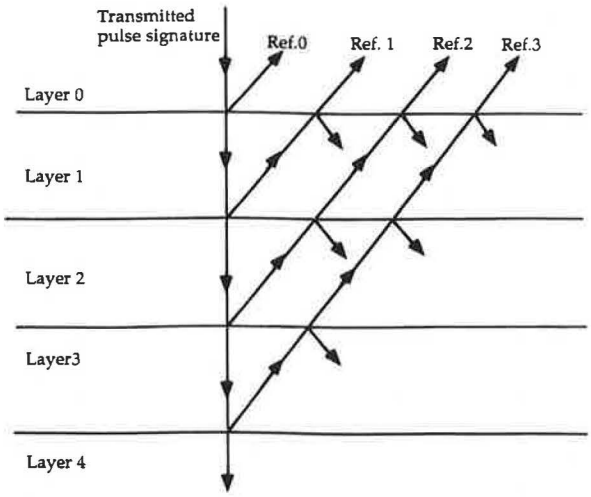

FIGURE 4 Paths of major reflection events.

model. Paths of these multiple reflection/transmission events are shown in Figure 5.

In the model proposed in this paper, no multiple reflections below Layer 2 are used. Layers 3 and 4 are subbase and subgrade in a pavement system; typically they hold significant amounts of moisture. Consequently, they have higher loss, and amplitudes from multiple reflections in these layers are negligibly small and are disregarded in the forward modeling process.

The pavements considered in this study are three-layer pavement systems (with two subsurface interfaces). Nevertheless, a four-layer pavement model is established in this study to account for special cases such as void and delamination between two adjacent layers. A three-layer model can be obtained from a four-layer model simply by using identical electrical parameters on two adjacent layers. Equations 5 and 6 are used to compute the attenuation and phase change on the pulse within each layer.

The amplitudes of the reflected and transmitted waves are determined by Equation pairs 8 and 10, and 9 and 11, respectively.

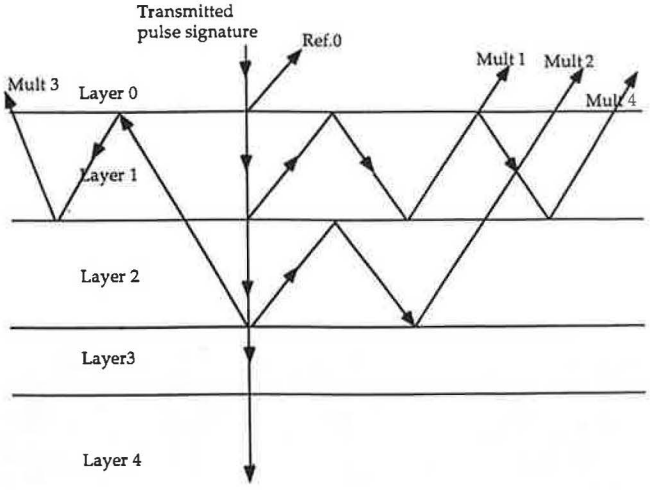

FIGURE 5 Selected paths of multiple reflection events.

Velocity of electromagnetic wave propagation in a medium with electrical parameters

$$\sigma = \sigma' + j\sigma'',$$
$$\varepsilon = \varepsilon' - j\varepsilon'', \text{ and}$$
$$\mu = \mu_0.$$

is expressed as (*4*)

$$v = c\left\{\frac{\left(\varepsilon' - \frac{\sigma''}{\omega}\right)}{2\varepsilon_0}\left[\sqrt{1 + \left(\frac{\varepsilon'' + \frac{\sigma}{\omega}}{\varepsilon' - \frac{\sigma}{\omega}}\right)^2} + 1\right]\right\}^{-1/2} \quad (12)$$

where $\mu = \mu_0$ is used because pavement materials are nonmagnetic. Because ω is large compared to σ' and σ'', and ε'' is small compared to ε', Equation 12 can be approximated by

$$v = \frac{c}{\sqrt{\frac{\varepsilon'}{\varepsilon_0}}} = \frac{c}{\sqrt{\varepsilon_r'}} \quad (13)$$

Using the thickness data and Equation 13, round-trip times for the three reflection events and four multiple reflection events can be determined in a three-layer system. Because each event generates a reflected pulse appropriately dispersed and attenuated, if these pulses are properly positioned according to their corresponding round trip times, a linear summation of the pulses produces the resultant synthetic waveform.

Summary of Forward Modeling Procedures

1. The GPR system is calibrated to obtain the transmitted pulse signature as it emerges from the antenna. The calibration procedure is as follows:
   - *a*. Set up the GPR system in an open environment with the antenna pointing to the sky. Record the end reflection signature of the GPR waveform (see Figure 6). This signal is essentially system noise; it will be present on all subsequent traces and should be removed.
   - *b*. Place a big (4 ft × 4 ft) flat metal plate perpendicularly below the antenna. The antenna should be mounted at the height to be used during normal operation, typically 12 in. Record the metal plate reflection (see Figure 7). The peak before the main peak is the end reflection measured in Step *a*.
   - *c*. Align and subtract the signature recorded in Step *a* from that of Step *b*. This provides a good approximation of the transmitted pulse of the monostatic GPR (see Figures 8 and 9).
2. Take the fast Fourier transform (FFT) of the transmitted pulse. Because the equations involved in the calculation of the model are frequency dependent, it is necessary to find the frequency components of the transmitted pulse. Figure 10 shows the frequency components of the transmitted pulse.

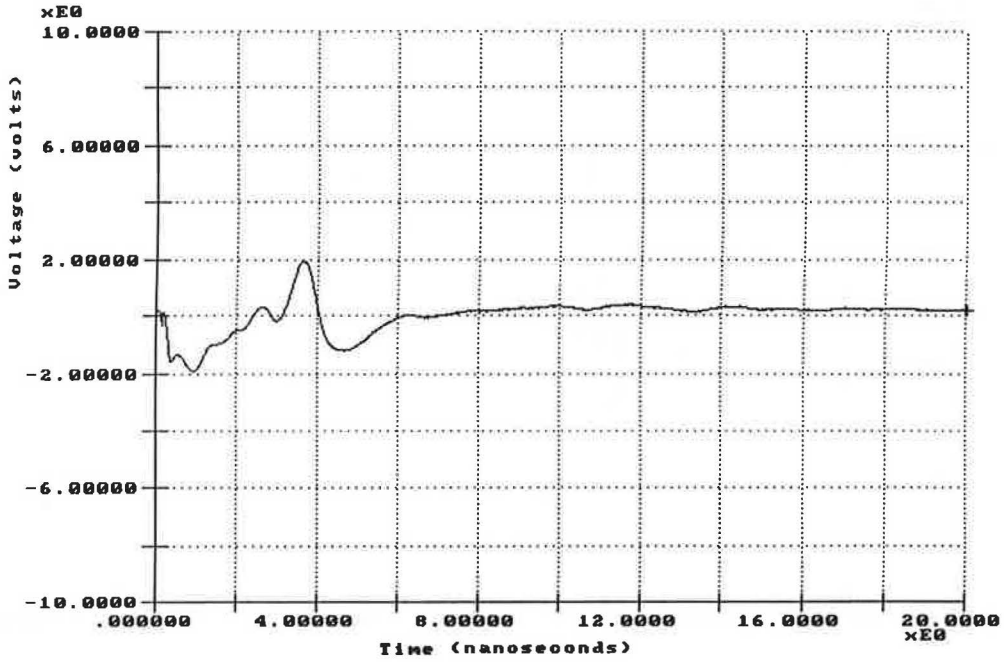

FIGURE 6 Signature of GPR waveform with antenna pointing skyward.

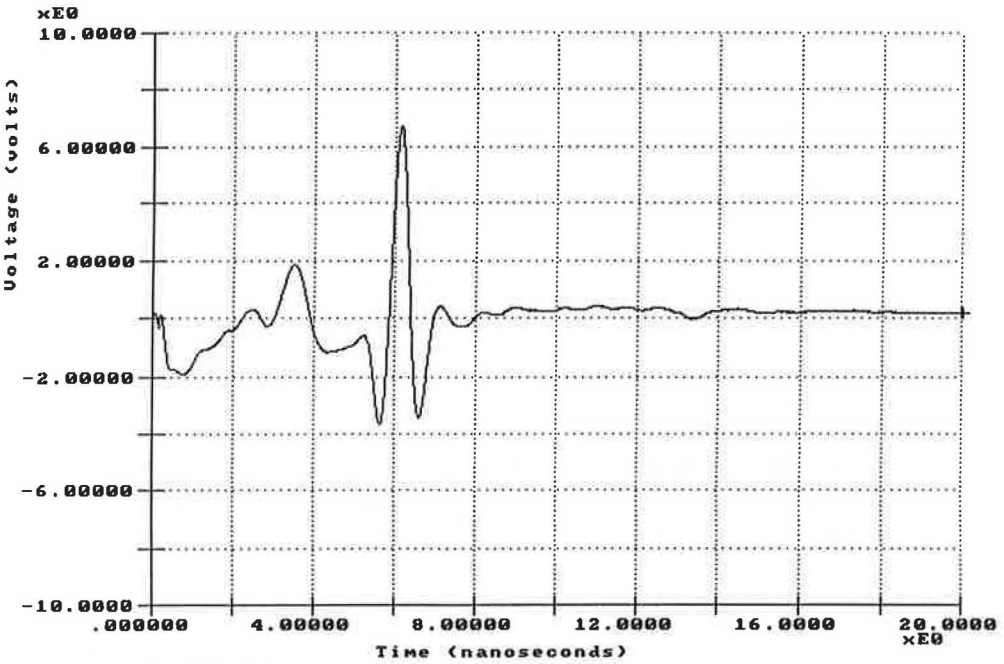

FIGURE 7 Signature of GPR waveform reflected from metal plate.

3. Consider an individual frequency component of the pulse as a continuous sinusoidal wave. Trace this wave through each of the selected ray paths and calculate all reflection, transmission, attenuation, and dispersion events encountered along each path. Do the same for all frequency components for each path. The amplitude and phase of the wave propagated through a path and reaching the pavement surface are expressed as a particular complex number characterizing the component of the pulse at that frequency. Consider these as new spectral elements of the spectrum. A resultant echo pulse is formed by taking the inverse FFT of the new spectrum.

4. Correct geometric spreading loss as discussed earlier.

5. Use Equation 13 to calculate the velocity of the GPR pulse in each layer. Calculate the time taken to propagate each of the paths in Step 3.

6. Position and superimpose each of the echo pulses according to the time obtained in Step 5 in the voltage versus time plot.

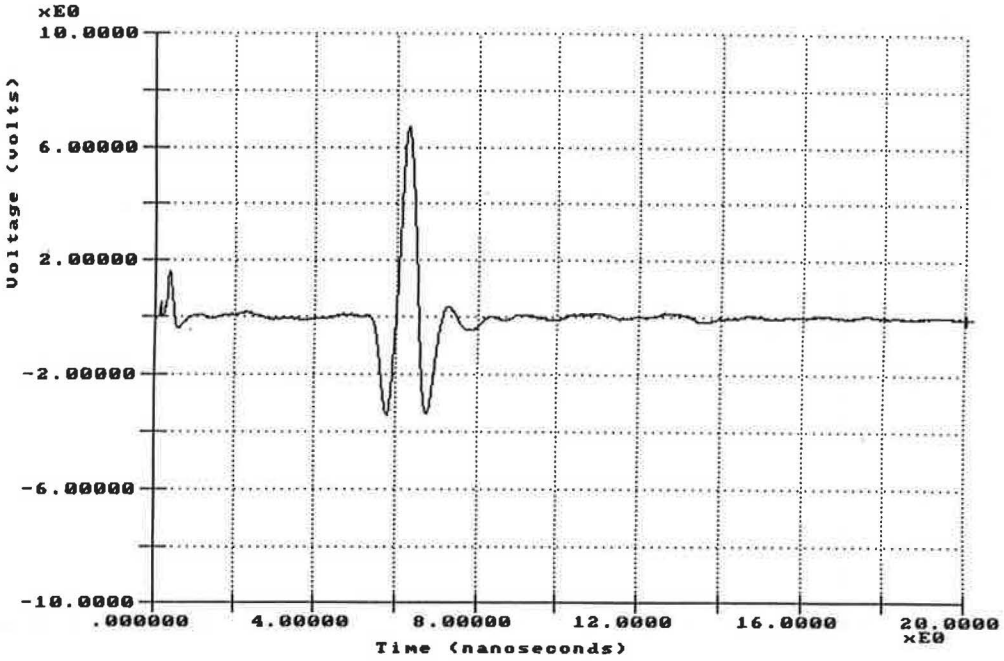

FIGURE 8 Result of waveform by subtracting Figure 6 from Figure 7.

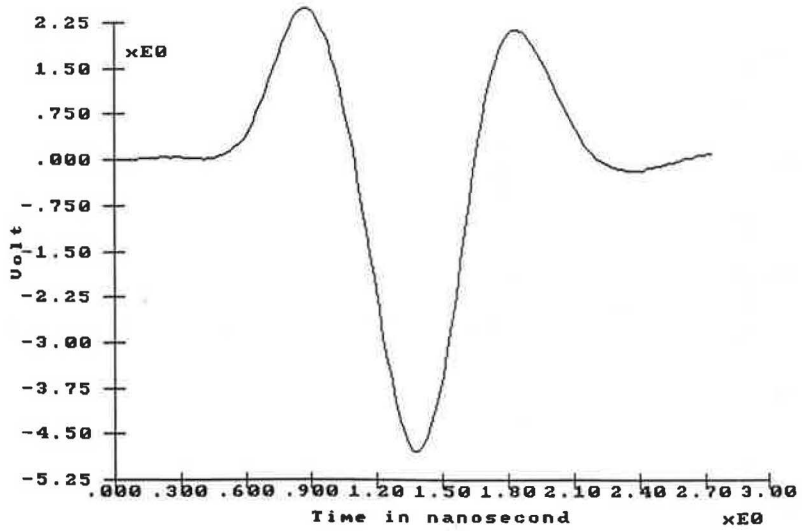

FIGURE 9 Transmitted pulse extracted from Figure 8.

Case Study

The forward model of a GPR trace provides a way to estimate the thickness of pavement layers. The idea is to objectively match the synthetic GPR trace and field GPR trace by altering iteratively the unknown parameters, which include the thickness of each layer, used in the model. After the synthetic GPR trace is obtained, the layer thicknesses used in the model are then taken to be the true layer thicknesses of the pavement. With some knowledge of the range of electrical parameters σ, ε, and μ in an individual layer, forward modeling can be an efficient method to determine the layer thickness.

The example field trace (Figure 11) is taken from a section of an experimental test pavement at the Texas Transportation Institute (TTI) Research Annex. The section is a three-layer pavement system. The theoretical and modeled GPR traces are shown in Figures 11 and 12, respectively. The measured and computed amplitudes and time delays between peaks are shown in Table 1 for comparison of these traces. Each amplitude is calculated by averaging the amplitude measured from peak to preceding minimum and peak to following minimum. The time delays are measured between peaks. The average error in predicting amplitudes is less than 9 percent, and in predicting time delays it is less than 2.5 per-

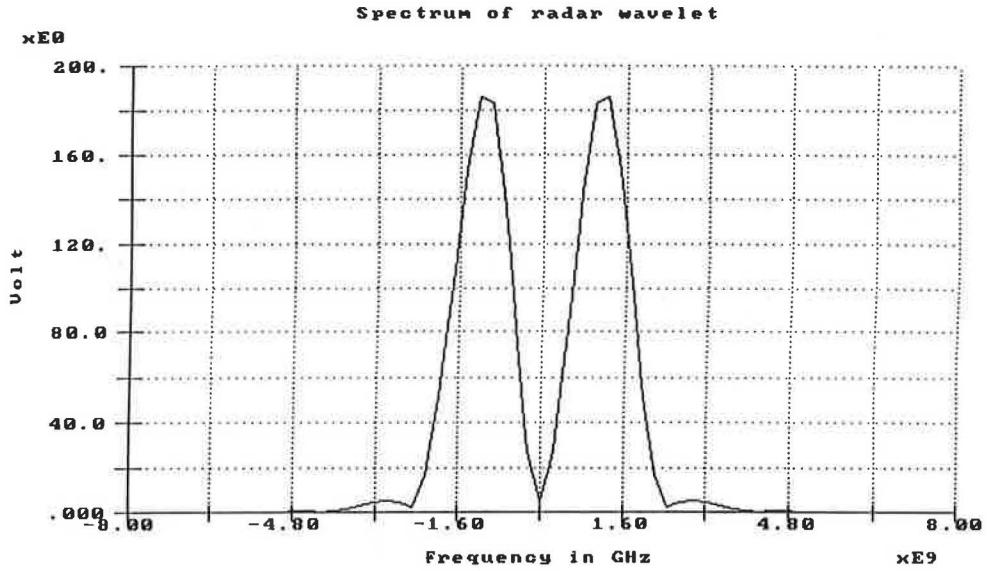

FIGURE 10 Frequency components of transmitted pulse.

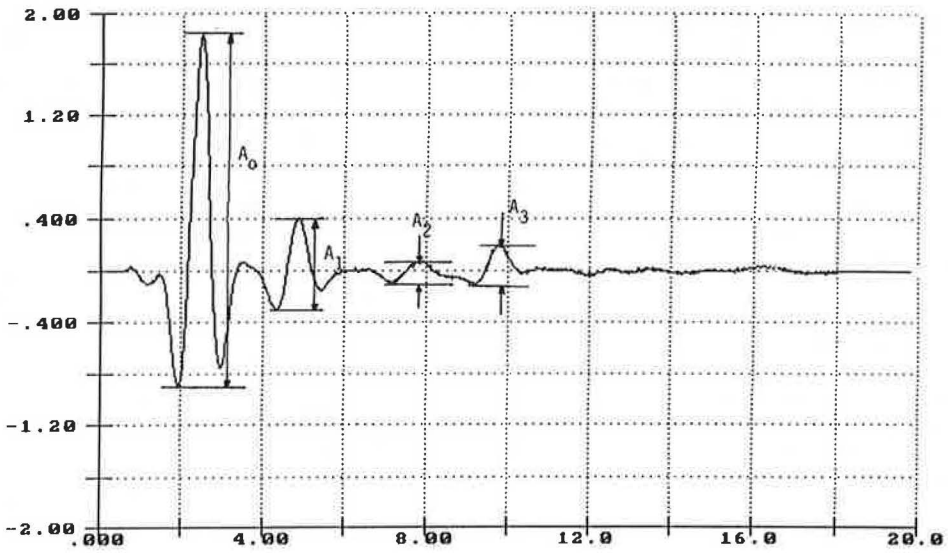

FIGURE 11 GPR field trace.

cent. A flowchart of the forward modeling process is shown in Figure 13.

Forward modeling can also be used to predict the signature of GPR traces taken from experimental or problematic pavement such as those with a void or delamination between two adjacent layers. Both water- and air-filled voids can be modeled. These simulations can be helpful to diagnosis of problematic pavements using GPR. Figure 14 shows the model trace resulting from the simulation of a three-layer pavement with an air void between concrete and base. The thickness of the void is ⅛ in. The thickness of the concrete and base layer are each 5 in. The dielectric values of concrete, base, and subgrade are 6.2, 9.6, and 10.5, respectively.

Once a match between the synthetic trace and the field trace is obtained, the electrical properties of the pavement subsurface are known. The synthetic trace is used for obtaining information of pulse amplitudes and round-trip times for layer thickness computations. The estimation of complex electrical properties of pavement materials is also provided by this model. The significance of these dielectric values for pavement engineers is as yet unknown. However, by applying constitutive models it may be possible to convert these values into more traditional items such as moisture content or void contents of pavement layers. This will be the subject of further research.

CONCLUSION AND RECOMMENDATIONS

A computer algorithm capable of simulating GPR waveforms collected from pavements was established. The pavement was modeled as a layered medium comprising layers of pavement

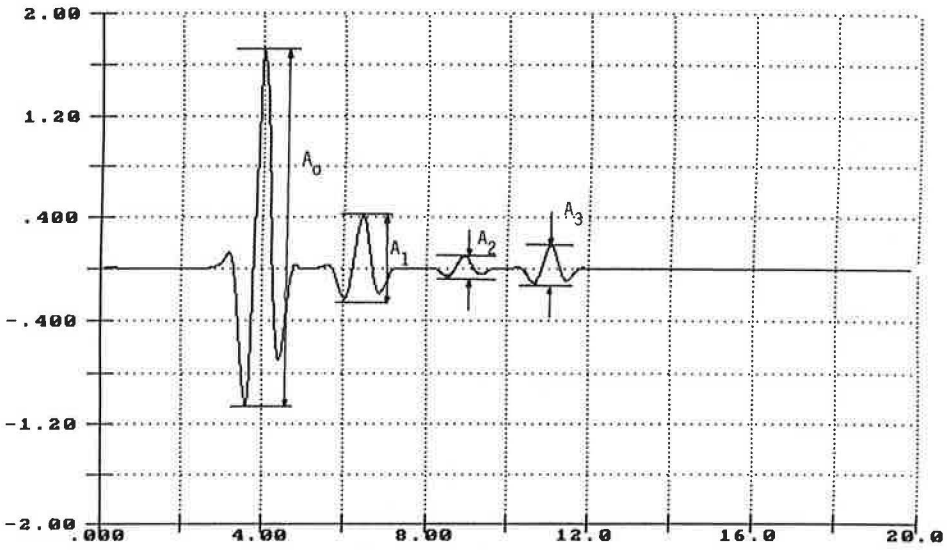

FIGURE 12 Corresponding forward model GPR trace.

TABLE 1 Comparison of Measured and Predicted GRP Traces

	Amplitudes (volts)				Time Delays (nanoseconds)		
	A_0	A_1	A_2	A_3	t_1	t_2	t_3
Model Trace	2.65	0.52	0.15	0.295	2.33	2.68	2.0
Field Trace	2.64	0.635	0.18	0.29	2.40	2.80	2.0
% error	0.4	17	16.7	1.7	2.9	4.3	0

where

A_0 is the amplitude reflected from surface.
A_1 is the amplitude reflected from top of base.
A_2 is the amplitude reflected from top of subbase.
A_3 is the amplitude reflected from top of subgrade.
t_1 is the round trip time to travel through the asphalt.
t_2 is the round trip time to travel through the base.
t_3 is the round trip time to travel through the subbase.

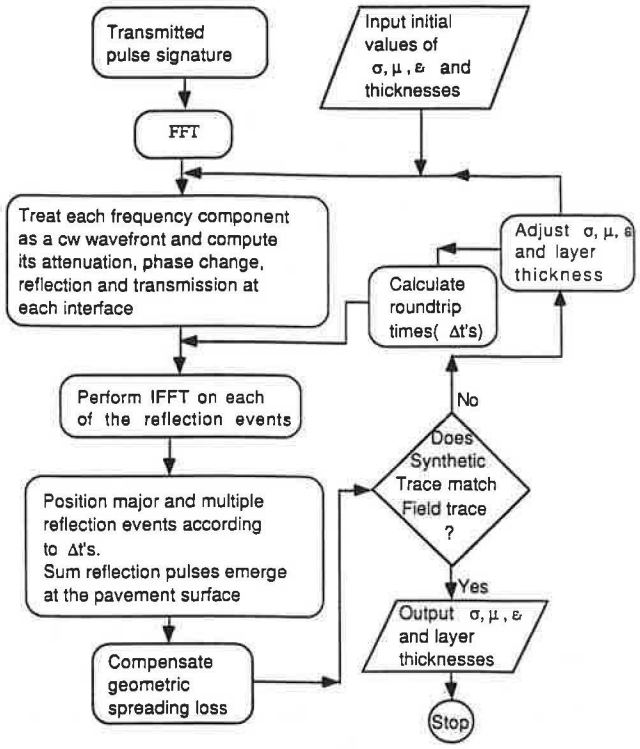

FIGURE 13 Flowchart of forward modeling.

materials. Two cases studies were carried out to investigate the feasibility of forward modeling in assisting pavement subsurface problems diagnosis. In the first case, the forward model was tested on data collected on experimental pavement of known layer thickness and types. Reasonable agreement was achieved between modeled and field traces. In the second case study, a ⅛-in. air void between concrete and base was simulated. These simulations computed ideal signatures of GPR waveforms collected from pavements with voids.

Recommendations for future work on related topics include the following:

1. Develop a least-square fitting algorithm to allow the model parameters (layer dielectrics and thicknesses) to be adjusted automatically by the computer until a satisfactory match between synthetic and field trace is achieved.
2. The accuracy of the complex dielectric constants of pavement materials is essential to the success of forward modeling. An initial guess that is too far away from the true values will affect the convergence toward a matching trace. Hence, more work is required in the area of measuring the complex dielectric and conductivity properties of paving materials for a range of materials and environmental conditions.

FIGURE 14 Model trace of three-layer pavement with air void between concrete and base.

REFERENCES

1. K. R. Maser and T. Scullion. Automated Pavement Subsurface Profiling Using Ground Penetrating Radar—Case Studies of Four Experimental Field Sites. Presented at 70th Annual Meeting of the Transportation Research Board, Washington, D.C., 1991.
2. W. J. Steinway, J. D. Echard, and C. M. Luke. *NCHRP Report 237: Locating Voids Beneath Pavement Using Pulsed Electromagnetic Waves,* TRB, National Research Council, Washington, D.C., Nov. 1981.
3. L. C. Bomar, W. F. Horne, D. R. Brown, and P. E. and J. L. Smart. *A Method to Determine Deteriorated Areas in PCC Pavements.* NCHRP Project 10-28 Final Report. TRB, National Research Council, Washington, D.C., Jan. 1988.
4. D. J. Gunton and H. F. Scott. Introduction to Subsurface Radar. *IEE Proceedings, Part F, Communications, Radar and Signal Processing,* Vol. 135, Aug. 1988, pp. 278–320.
5. R. F. Harrington. *Time-Harmonic Electromagnetic Fields.* McGraw-Hill Book Company, New York, N.Y., 1961, p. 38, Equation 2-8.
6. S. Duke. *Calibration of Ground Penetrating Radar and Calculation of Attenuation and Dielectric Permittivity versus Depth.* M.S. thesis. Colorado School of Mines, Golden, June 1990.

Publication of this paper sponsored by Committee on Pavement Monitoring, Evaluation, and Data Storage.